ROUGHNESS TRANSFER MODEL BASED ON THE MONTE CARLO METHOD: APPLICATION TO STEEL SHEET TEMPER ROLLING*

Nicolas LEGRAND[1]
Christian COUNHAYE[2]
Nelson SOUTO[1,3]
Don EARLEY[4]
Matt SZIDON[4]

Abstract

The work is motivated by the automotive customer requirements for a roughness with high peak density (RP_c > 75 peaks/cm) on steel sheet surfaces to maintain a good strip surface finish after painting. For that purpose, a new approach is utilized to compute roughness transfer and predict final roughness on uncoated steel sheets (average roughness, skewness, peak density) as a function of temper rolling conditions. The approach is based on the Monte Carlo method combined with the Abott curves and an auto-correlation function to numerically generate roughness profiles for roll and strip respectively. To compute the roughness transfer due to the interaction between roll and strip surfaces during rolling, a composite Abott curve that combines roll and strip Abott curves is used with an asperity crushing model integrated with a rolling model. This enables simulating two roughness transfer mechanisms in the roll bite: the strip asperity crushing mechanism by roll roughness and the strip asperity ploughing mechanism due to roll-strip interfacial sliding speed. The model shows the importance of considering the two mechanisms to predict roughness transfer correctly when strip elongation is high, typically a few percent, and roll bite friction is low. In these conditions, the forward slip at the exit of the roll bite tends to erode strip roughness significantly and decrease considerably the peak density on the strip. For lower elongation levels (~1%) and high roll bite friction, the ploughing mechanism becomes negligible and roughness transfer is controlled by the crushing mechanism only. With these two mechanisms, the model reasonably predicts the evolution of average roughness and peak density over a wide range of temper rolling conditions (new/worn work rolls, hard/soft grades, various elongations), but skewness is more difficult to predict for some trials.

Finally, the model is used to evaluate some process parameters to maximize peak density out of the temper mill to meet the challenging automotive customer peak density requirements of 75 peaks/cm.

Keywords: Monte Carlo Simulation, Abott curves, Roughness transfer, Temper rolling; Peak Density

[1] *ArcelorMittal Global R&D East Chicago, IL 46312, USA.*
[2] *Consultant, B-4845 Jalhay, Belgium.*
[3] *Now at ArcelorMittal Global R&D Maizieres, 57283, France*
[4] *ArcelorMittal Nippon Steel Sumitomo JV, Calvert, AL 36513, US*

Nomenclature

R_a, R_{sk}, RP_c: average roughness, skewness, peak density (peak/cm) parameters
ACF, β^*, P_c: Auto-Correlation function, Auto-correlation distance, Correlation factor ($0<P_c<1$)
A_{entr}, A_{roll}, A_{co}: Abott curves for incoming strip (entry), roll and composite (strip + roll) respectively

1. BACKGROUND – STATE OF THE ART

1.1 Problem definition

Roughness transfer remains one important quality aspect for steel sheet products. It is usually obtained by texture transfer from roll to strip at the last stand of the tandem cold mill or at the temper mill.

Steel sheets for tin plate applications may require a roughness with a negative skewness (R_{sk} < 0: fig. 2) after temper rolling to favor a hydrostatic pressurization of lubricant pockets during the subsequent deep drawing process. This hydrostatic pressurization further activates micro-plasto-hydrodynamic lubrication **[1]**. Steel sheets for automotive applications may require high peak density (RP_c > 75 peaks/cm) after temper rolling, in addition to the usual average roughness R_a, to maintain a correct surface finish after painting.

Therefore, roughness transfer modeling during cold and temper rolling is necessary to better understand the interaction between roll and strip surfaces and to predict final strip roughness to meet the quality aspects required by customers.

1.2 Abott curve for surface roughness

An Abott curve characterizes the roughness profile of a surface. It defines the evolution from 0 to 1 of the contact ratio A when the indentation plan cuts the roughness profile from highest peaks (A=0) to deepest valleys (A=1) (figure 1).

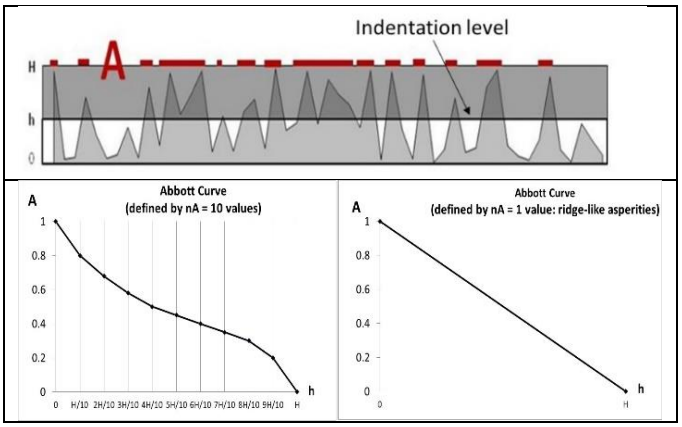

Figure 1. Abott curve. Top: definition of A and h (smooth roll / rough strip). Bottom: example of Abott curves A(h) for two different roughness profiles.

1.3 Existing roughness transfer models

Roughness and texture transfer modeling have been extensively investigated in literature **[2,3,4,5]**: the studies focus on roughness transfer modeling due to the roll indentation into the strip. Moreover, these works usually model the vertical distribution of peaks of asperities only and the associated roughness parameters R_a, R_{sk}, R_q. But the horizontal distribution of peaks associated to RP_c is ignored.

Finally, none of these works consider the interfacial roll-strip sliding in the bite and its potential influence on roughness.

More recent works like **[6]** attempted to model this sliding of roll onto the strip, which is the main source of the ploughing mechanism. These approaches are costly in computing time as they require the full finite element method to accurately capture the complex plastic deformation coming from the roll-strip interaction.

However, it is unclear if and how much the ploughing mechanism of asperities affects roughness transfer in temper rolling.

1.4 Objectives of the present work

Based on the previous analysis, the primary objective of this work is to develop a model that simultaneously computes the vertical (R_a, R_{sk}, R_q) and horizontal (RP_c) distribution of peaks during temper rolling. Secondly, the ambition is to address if, how and how much the ploughing mechanism due to interfacial sliding affects the texture transfer in the bite during rolling, in addition to the indentation mechanism.

2. ROUGHNESS TRANSFER TRIALS

2.1 Trials conditions

10 coils have been selected for the roughness transfer trials at the Hot Dip Galvanizing line nº2 of AM/NS Calvert plant. Table 1 summarizes grades, thicknesses and widths for these 10 trial coils. The AM/NS galvanizing line produces only uncoated steel sheets and

the 10 selected coils are unexposed. Two different skin pass mills have been used for the trials: the inline skin pass and the stand-alone off-line skin pass. The stand-alone skin pass offers more flexibility to perform trials with different elongations along the coil while the inline skin pass provides more industrial conditions for roughness transfer.

Table1: coils for roughness transfer trials

Coil No	Coil ID	Steel Grade	Thickness [mm]	Width [mm]
#1		HSLA	1.211	1112
#2		HSLA	0.757	1415
#3	2203413180	IF	0.798	1530
#4		HSLA	0.679	1530
#5	2203416710	IF	0.885	1081
#6	2203416700	IF	0.885	1083
#7	2203416700	IF	0.885	1083
#8	2203416710	IF	0.885	1081
#9	2203423120	IF	0.755	1467
#10	2203416710	IF	0.885	1081

Coil #5 and coil #8 are from the same mother coil. Coils #6 and #7 are also from the same mother coil. Coils #5, #6, #7, #8 are exactly same grades, same thickness, same width. Coil #10 = coil #8 re-skin passed a 2nd time at the stand alone skin pass.

Different combinations of temper rolling passes have been made with these two skin pass mills: stand-alone skin-pass only, inline skin-pass only, inline followed by stand-alone skin-pass rolling.

Moreover, different temper rolling conditions have been used: new/worn work rolls, soft/hard grades (IF and HSLA grades), various elongations. Finally for the stand alone skin pass, work rolls with different roughnesses have been manufactured by EDT (Electro-Discharge Texture).

Figure 2 shows the correlation between R_a and peak density measured on the rolls of the stand alone skin pass: the higher roll peak density is, the lower roll Ra is.

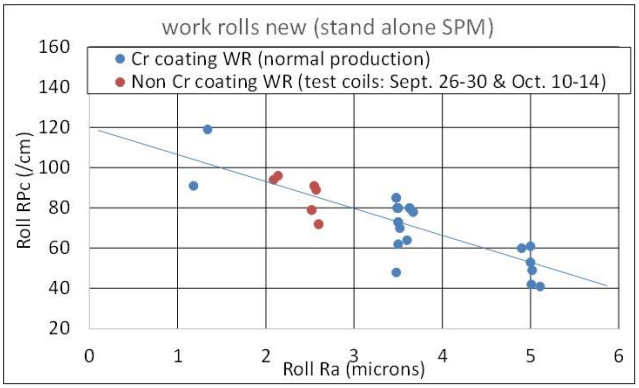

Figure 2. measured roll Ra and roll peak density for the different rolls used for trials

This correlation is due to the slope of roll asperities that remains unchanged whatever roll R_a is: a lower R_a generates a higher peak density (fig. 3).

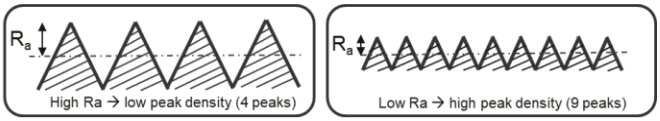

Figure 3. geometrical correlation between R_a and peak density (peak count/cm). Left: high Ra, low peak density; right: low Ra high peak density

The roughness parameters measured during the trials are the average roughness R_a (amplitude of the roughness profile), the skewness R_{sk} (asymmetry of the roughness profile) and the peak density (fig. 4).

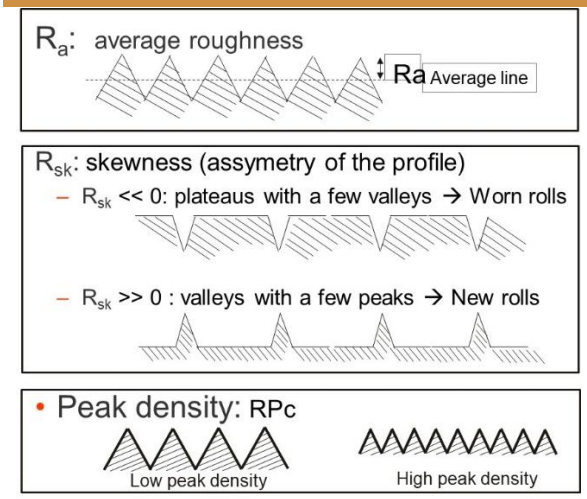

Figure 4. The 3 roughness parameters R_a, R_{sk}, peak density considered in this study.

Roll roughness was measured along the roll axis with a Jenoptik Hommel W10 profilometer before and after each trial coil (fig.5 top) with the following conditions: L_t = 15 mm (measurement length), cut-off = 2.5 mm, threshold = +/-0.5 μm).

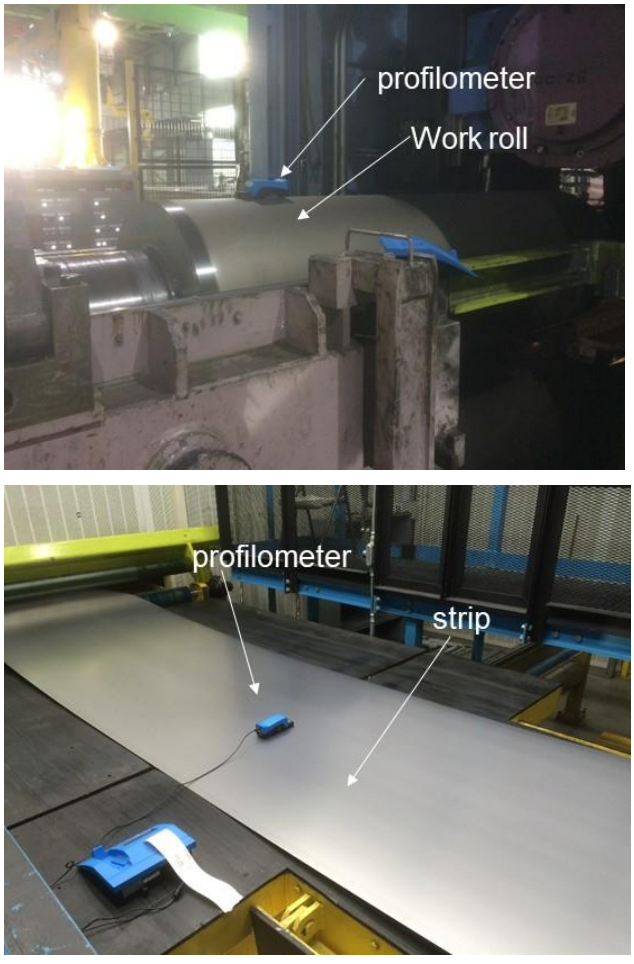

Figure 5. top: roll roughness measurement – bottom: strip roughness measurement

Before and after each trial, coils were uncoiled on an inspection line and strip roughness was measured using the same profilometer at different positions along the strip in the rolling (0º) and in the transverse (90º) directions (fig.5 bottom).

2.2 Trials results

Figures 6 and 8 show the strip roughness (R_a, R_{sk} and peak density) measured along the coils #1 to #9 for IF and HSLA grades at HDGL2 exit but before the stand alone skin pass rolling. The roughness measured on coils #1, #3 and #4 corresponds to tandem mill exit roughness (no elongation at inline skin pass.

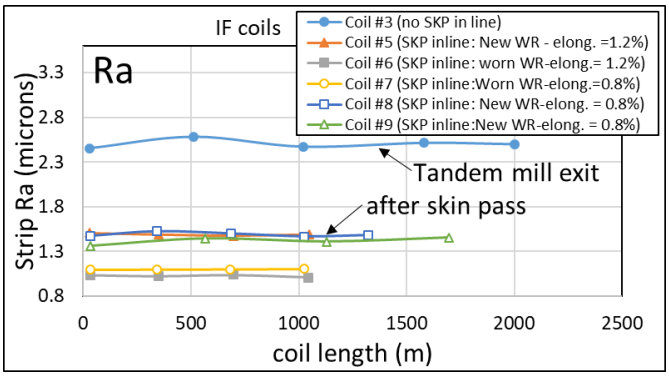

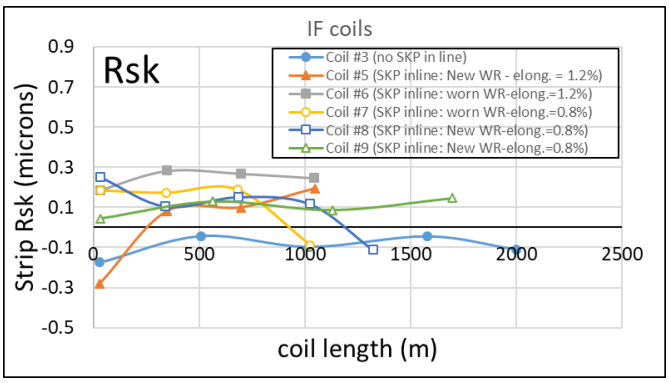

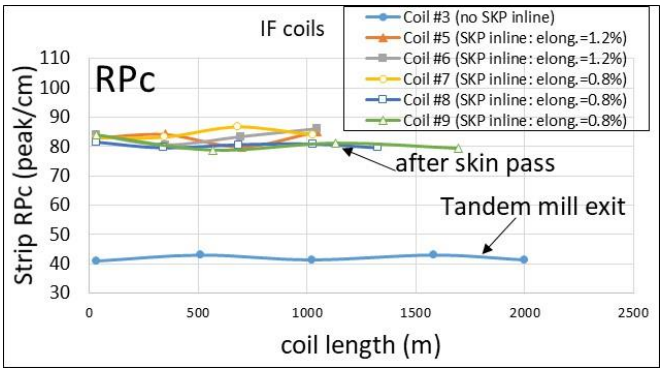

Figure 6. strip roughness measured along IF grade coils (table 1) with/without inline skin pass elongation (no stand alone skin pass)

From these measurements, the following conclusions can be drawn:

-strip roughness (R_a, RP_c) is relatively uniform along the coils.

-strip skewness R_{sk} out of tandem mill (before skin pass) is positive (coils #1, #4: fig.8) or negative (coil #3: fig.6). This difference might be due to the difference of roll wear at the tandem mill exit between these different coils: coil #3 was rolled with new rolls (R_{sk}>>0) at tandem mill exit which tends to imprint a negative R_{sk} on the strip. While coils #1 and #4 were rolled with worn rolls (R_{sk} <<0) at tandem mill exit which tends to imprint positive skewness R_{sk} on the strip as illustrated on figure 7.

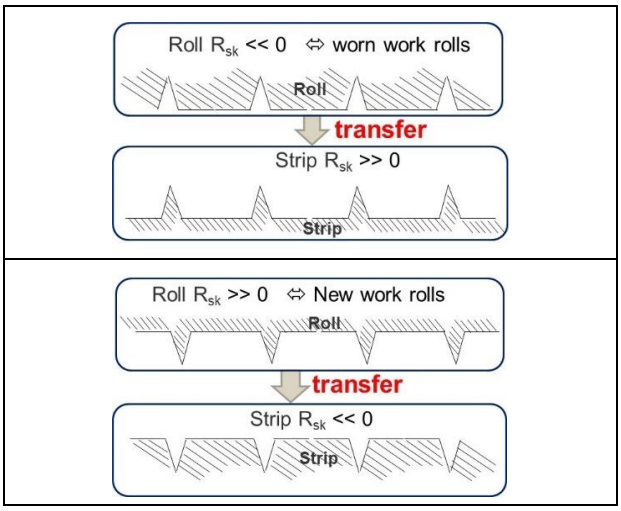

Figure 7. illustration of R_{sk} skewness sign imprinted on the strip as a function of roll R_{sk} skewness sign that depends on roll wear level. Top: worn rolls, bottom: new rolls

-Wear level of work rolls influence strip R_a significantly but not really the strip peak density: coil #7 versus coil#8 (fig. 6). The higher the roll wear is, the lower the R_a transfer on the strip is (decrease by ~50% between worn and new work rolls).

-Elongation increase from 0.8% to 1.2% (within customer tolerance) at inline skin pass does not modify noticeably roughness transfer out of skin pass mill: coil #6 versus coil #7 or coil #5 versus coil #6 (fig.6). Elongation change must be significantly higher to modify noticeably roughness transfer on the strip (see section 4).

-Roughness measured on coil #3 which has not been temper rolled at the inline skin pass (fig. 6), is the roughness made on the last stand of the tandem mill. For this coil, strip peak density is particularly low (42 peaks/cm) and as a consequence strip Ra is high (~2.5 μm), confirming the trend of figure 2. This low strip peak density is due to a transfer of a low roll peak density (45 peaks/cm) as measured on rolls.

For this coil #3, strip R_a~2.5 μm is much higher than the roll R_a~1.5 μm of the tandem mill. This unexpected result has not been investigated further with the model due to lack of rolling data from the tandem mill.

Figure 8 for HSLA grade confirms figure 6:

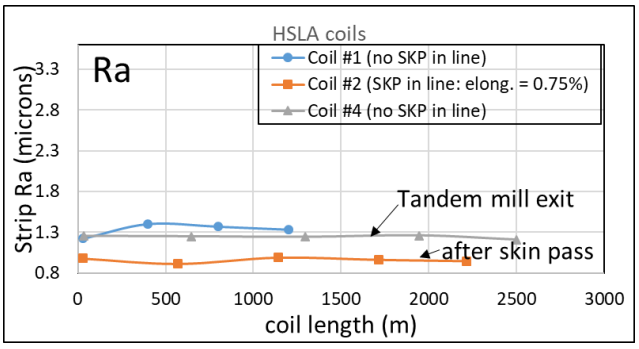

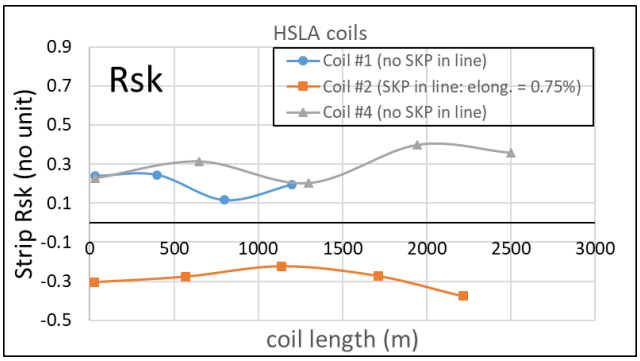

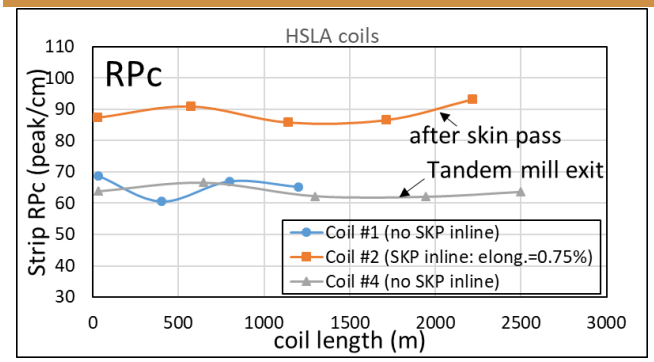

Figure 8. strip roughness measured along HSLA grade coils (table 1) with/without inline skin pass elongation (no stand alone skin pass)

-roughness measured on coils #1 and #4 (no inline skin pass) corresponds to roughness from the tandem mill: the RP_c of 65-70 peaks/cm (coil #1) is close to the roll RP_c of ~75 peaks/cm of the last stand tandem mill work roll. The strip Ra of 1.2-1.4 μm is similar to the Ra ~1.4 μm of the last stand tandem mill work roll.

-the high RP_c (~90 peaks/cm) measured on coil #2 skin passed on the inline skin pass (fig.8), is due to the high RP_c of inline skin pass work rolls: RP_c = 89 peaks/cm was measured on work roll for coi l#7 which has similar conditions as coil #2.

-the Ra~1.2/1.4 μm measured on coil #2 is close to the work roll Ra of the inline skin pass measured at 1.51 μm for coil #7 that is similar to coil #2.

As a conclusion, the above experimental results show that roll wear has a significant influence on strip R_a, much less on strip peak density. Moreover, an elongation increase within the customer tolerance (0.8 to 1.2%) does not impact roughness transfer. Finally, the strip roughness out of the tandem mill can vary a lot depending on the roll wear level of the last stand of the tandem mill. This variability needs to be evaluated with the roughness transfer model presented in the next section.

3. ROUGHNESS TRANFER MODEL

3.1 Monte Carlo method

The Monte Carlo method **[7]** is used in the model to generate numerical roughness profiles for roll and strip surfaces. These numerical profiles are a set of random heights separated by a distance 'space-step' which is the mesh of the profile (figure 9).

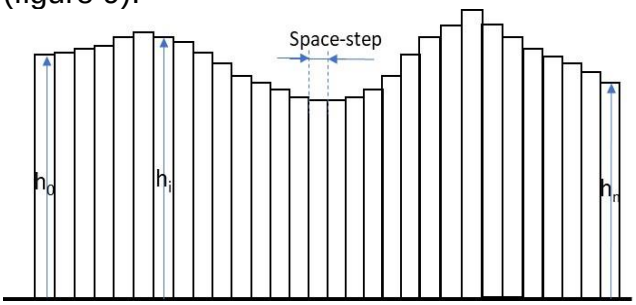

Figure 9. Illustration of numerical roughness profile generated by the Monte Carlo method: h_0 to h_n are peak heights respecting the Abott curve and the Peak density measured on the physical surface

The Monte Carlo method determines the random heights that satisfy both the Abott curve (vertical distribution of peaks) and the peak density (horizontal distribution of peaks) that were measured on real roughness profiles collected on roll and strip during the trials.
Below is detailed how this Monte Carlo method is used with the Abott curves and the auto-correlation function to generate the profiles:

Abott curve

The vertical distribution of peaks is computed by generating a set of random values A* that follows a uniform distribution between 0 and 1, and by taking the corresponding profile heights h* from the Abott curve. This creates a set of random heights that satisfy the statistics of asperity heights of the Abott curve measured on the surface.

Auto-Correlation Function (ACF)

To compute the horizontal distribution of peaks and satisfy also the peak density (RP_c) measured on the surface, it is necessary to use an Auto-Correlation Function (ACF) to introduce some degree of correlation in the above generation of random numbers A*.

This degree of correlation reflects the fact that if a certain node in the profile corresponds to a peak, there is a higher probability that the next node in this profile corresponds also to a peak rather than a valley. The higher this correlation is, the lower the peak number per centimeter is.

The introduction of this correlation in the generation of the profile is made through the following equation:

$$A_0^* = random\ number = rand\ num \in]0,1[\qquad (1)$$
$$A_{i+1}^* = \phi_{0,1}\left[(1-P_c^2)^{1/2}.\phi_{0,1}^{-1}(A_i^*) + P_c.\phi_{0,1}^{-1}(rand\ num \in]0,1[\,)\right]$$

In equation (1), the current random number A_i^* (gaussian variable) is combined with the new random number 'rand num' (gaussian variable) using the respective factors $(1-P_c^2)^{1/2}$ and P_c so that the new random number A_{i+1}^* is also a gaussian variable. This processus using the Gauss distribution function enables to combine successive random numbers with a certain correlation in between to build the complete profile.

Therefore, equation (1) expresses the relationship between the random number A_{i+1}^* of the next point and the random number A_i^* of the actual point in the profile. Therefore, this equation enables to calculate the random numbers A* over the complete roughness profile with a certain degree of correlation between two successive points of the profile.
$\phi_{0,1}$, the Gauss distribution function, is classically used to introduce correlation in the Monte Carlo method. It has the following expression:

$$\phi_{0,1}[x] = \frac{1}{\sqrt{2.\pi}}.\int_{-\infty}^{x} e^{\frac{-1}{2}t^2}.dt \qquad (2)$$

P_c is the correlation factor ($0<P_c<1$):
<u>P_c=0:</u> $A_{i+1}^* = A_i^*$, there is no height variation from one node to the next one, the profile is flat.
<u>P_c=1:</u> $A_{i+1}^* = random\ number \in]0,1[$, uncorrelated with A_i^*, in this case the peak count is maximum.

With the above equations, the heights of two successive points in the Monte Carlo profile are correlated with a coefficient:

$$R = (1-P_c^2)^{1/2} \qquad (3)$$

It means that two points with a distance of n nodes (n space-steps) are correlated with a coefficient R^n. The auto-correlation function is the correlation between one profile and the same profile shifted by a distance β = n.space-step. Therefore the expression of the auto-correlation function in this model is:

$$(1-P_c^2)^{n/2} \qquad (4)$$

Auto-correlation distance

The degree of correlation of the profile is quantified by the auto-correlation distance β^* (e.g. the distance over which the profile is considered no longer correlated with itself). A usual expression for the auto-correlation function is a decreasing exponential function $e^{-\beta/\beta*}$ **[8]**. Equating $e^{-\beta/\beta*}=(1-P_c^2)^{n/2}$, with β=n.space-step, then the auto-correlation distance β^* is defined by:

$$\beta^* = \frac{-2}{Ln(1-P_c^2)}.space\_step \qquad (5)$$

This length is approximately a fraction (~¼ to $1/5$) of the distance between two peaks as shown with the following application:
Space-step = 0.01mm, P_c = 0.53 correponding to RP_c=43 peaks/cm (fig. 11), so distance between 2 peaks = 232 μm): the auto-correlation distance = 6.06*space-step = 60 μm ~ ¼ x 232 = ¼. distance between 2 peaks. So the auto-correlation distance is realistically a fraction of the distance between peaks.

Monte Carlo method application

The above Monte Carlo processus is applied here to a physical roughness profile that has been measured on a steel sheet after cold rolling at tandem mill (figure 10).

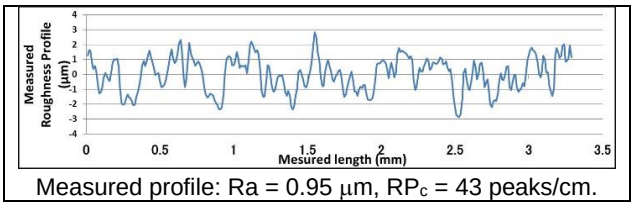

Measured profile: Ra = 0.95 µm, RP_c = 43 peaks/cm.

Figure 10. physical roughness profile measured on uncoated steel sheet at cold tandem mill exit.

Using equation (1), random profiles are generated with a space-step = 0.01 mm and different values for the correlation factor P_c.

It gives the following peak density versus Pc (fig. 11-a): selecting a P_c=0.53 enables the Monte Carlo profile to target the measured peak count RP_c = 43 peaks/cm (figure 10). It is also verified that the Monte Carlo Abott curve for P_c = 0.53 describes the Abott curve from the measured profile (fig. 11-b).

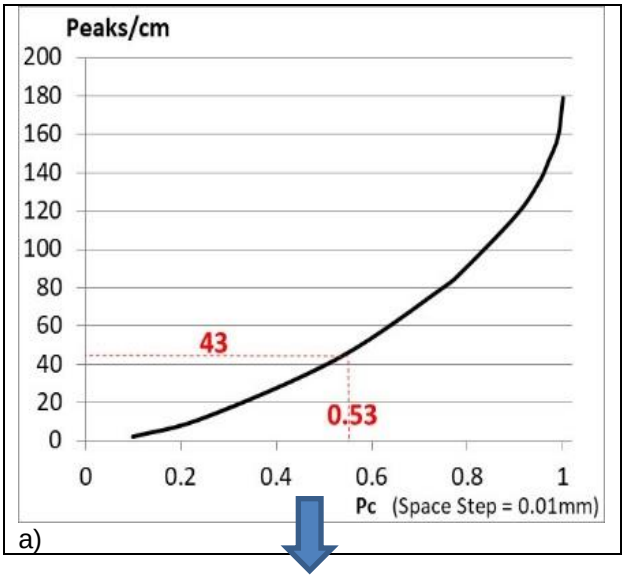

a)

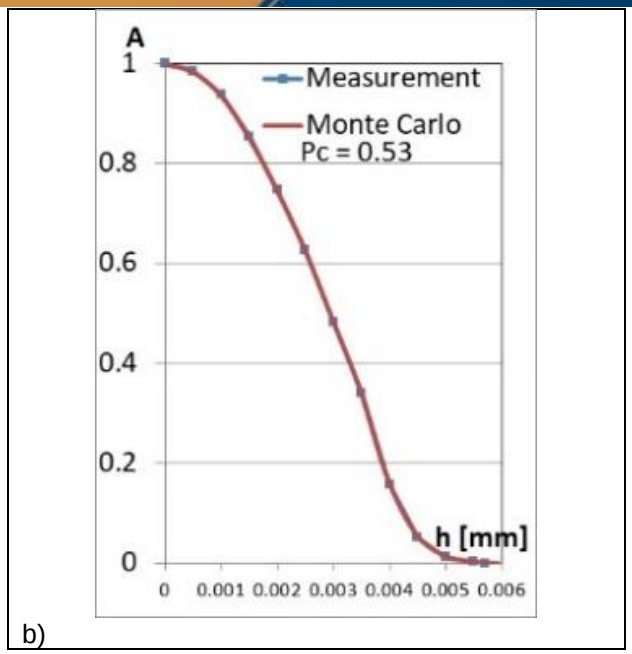

b)

Figure 11. a) peak density for different P_c values. b) Abott curve from measured (fig.8) and Monte Carlo profiles (fig.10).

Figure 12 shows two different numerical roughness profiles randomly generated by Monte Carlo and using two different P_c and space-step parameters.

These two profiles have the same roughness parameters and Abott curve as the measured profile of figure 10.

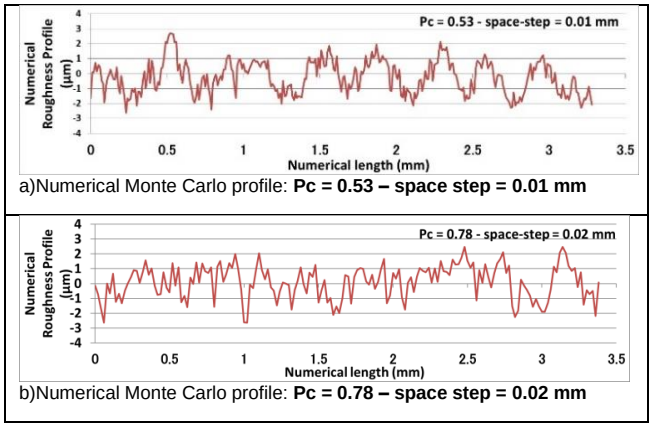

a)Numerical Monte Carlo profile: **Pc = 0.53 – space step = 0.01 mm**

b)Numerical Monte Carlo profile: **Pc = 0.78 – space step = 0.02 mm**

Figure 12. Numerical Monte Carlo roughness profiles using two different P_c and space steps values and equivalent to the physical profile of fig.10.

3.2 Roughness transfer computation

Roughness transfer by indentation [5]

(roll-strip indentation without sliding)

Once the profiles for roll and strip have been numerically generated by Monte Carlo, their roughness is described by their respective Abott curve A_{entr} and A_{roll} (fig.1).

The interpenetration of these two rough surfaces (vertical direction) is described by the composite Abott curve A_{co}.

This curve is the combination of the incoming strip Abott curve A_{entr} and the roll Abott curve A_{roll}. Its aim is to establish a relationship between the contact ratio A and the average distance h between the two rough surfaces in contact. The composite Abott curve equation is defined by **[5]**:

$$\mathrm{Aco(h)} = \int_{h}^{Hentr+Hroll}(-\mathrm{dAco(h')/dh')}\,.\,\mathrm{dh'} = \int_{h}^{Hentr+Hroll}\left(\int_{0}^{Hentr}\mathrm{dAentr(h'')/dh''}.\mathrm{dAroll(h'-h'')/dh'}\,.\,\mathrm{dh''}\right).\mathrm{dh'} \quad (6)$$

Figure 13 shows the roll, strip and composite Abott curves for the trial #6.

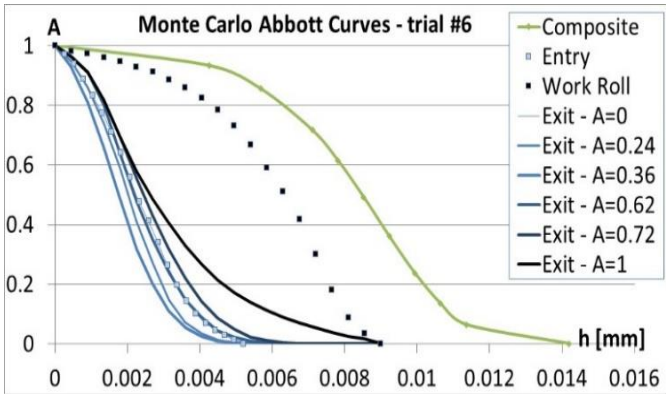

Figure 13. Abott curves obtained by Monte Carlo for roll, for strip entry, for strip exit at different contact ratio A and for composite – trial #6 (table 1).

This composite Abott curve is then used with the asperity crushing model of Wilson **[9]** to compute the contact ratio A_{co} resulting from interpenetration of the two surfaces. A_{co} is a function of the average pressure $\bar{p}$ at the contact between roll and strip. This average pressure is given by the rollgap computation calculated with the rolling model **[5]**. There are strip plastic and strip elastic zones along the roll bite, so two equations are used to compute the contact ratio evolution along the contact **[10]**:

-Elastic zone: $A = f(\overline{p})$ (7)

When bulk of the strip does not plastify (e.g. last stand of tandem cold mill), the roughness transfer is governed by the average pressure $\bar{p}$ and strip asperities resist strongly to roll indentation.

-Plastic zone: $dA/d\epsilon_y = f(A, \bar{p})$ (8)

When plastification of the bulk occurs, the contact ratio A depends on the reduction $d\varepsilon_y$. Here strip asperities have a much lower resistance to roll indentation.

It must be highlighted that the progressive indentation of the roll into the strip in the crushing model is made under the assumption that the Abott curve of the strip remains unchanged. This assumption implies that the sheet material disappears during the crushing of its peaks by the roll, as illustrated by the red areas on figure 14. So the mass of material is not conserved.

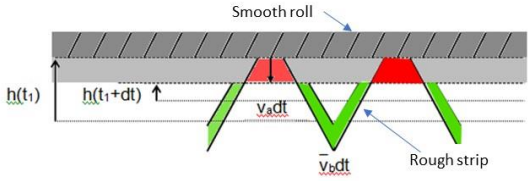

Figure 14. illustration of progressive crushing of a rough strip (saw touth roughness) by a smooth roll.

Therefore, to conserve the mass of material, the following kinematic assumption is made: the surface of valleys is subjected to a uniform upward motion (green area on figure 14) to compensate for the red areas disappearance in the contact areas where the roll crushes the strip peaks. As a consequence, with this assumption the mass of material is conserved during crushing (red area = green area).

Figure 15 illustrates the progressive indentation based on the mechanism of figure 14: here, both roll and strip surfaces are rough during indentation. Moreover the roll imposes its roughness profile to the

strip since the roll is much harder than the strip. For this roughness computation, the roll is supposed rigid and the strip perfectly plastic: strip peaks are crushed by the roll and strip valleys evolve until the strip surface is in full contact with roll roughness.

On figure 15, the Abott curves are also considered unchanged during indentation of the roll into the strip, which does not allow to conserve the mass of material.

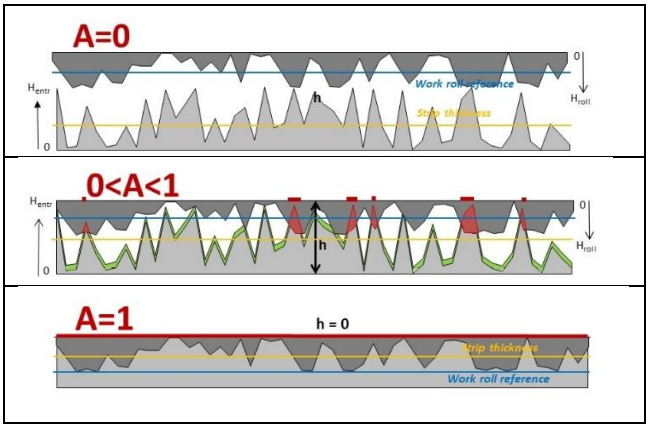

Figure 15. illustration of progressive penetration of roll roughness into the strip roughness and contact ratio evolution as considered by the model: Top: no contact, middle: partial contact, bottom: full contact roll-strip

So similarly to figure 14, the sheet material in the contact areas with the roll which disappears by crushing (red areas) is compensated by a uniform upward motion of free surfaces in the valleys (green areas) so that the mass of material is conserved (read area = green area).

In reality, the roll is plastically deformed during indentation. However this mechanism is included in the roll wear that is considered in the model by measuring roll roughness after rolling. Moreover, the roll and the strip are elastically deformed but these elastic strains have been estimated to a 5% decrease of roughness peaks (~10% in total for roll and strip), which is neglected in the model.

Roughness transfer by ploughing

(roll-strip indentation and sliding)

When strip elongation is sufficiently high (generally greater than 1%) and roll bite friction relatively low, the sliding between roll and strip surfaces is no longer negligible on roughness transfer and must be considered by the model.

Figure 16 illustrates this sliding mechanism, called ploughing, where the contact ratio is approximately divided by 2 in the sliding situation compared to the sticking situation (indentation).

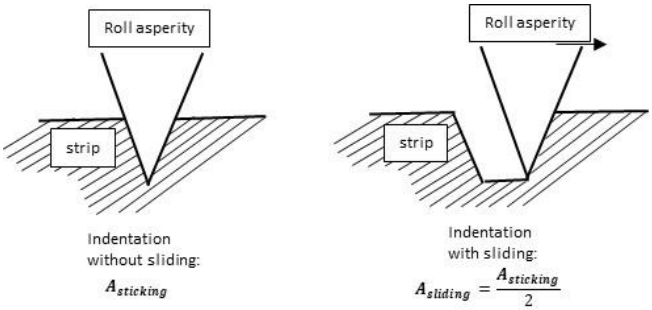

Figure 16. crushing (left) and ploughing (right) mechanisms: when sliding of roll asperities onto strip surface, the contact ratio is decreased.

Figure 17 shows schematically the different zones of the roll bite calculated by the rolling model and in particular the two sliding zones (entry/exit) and the central sticking zone (no sliding).

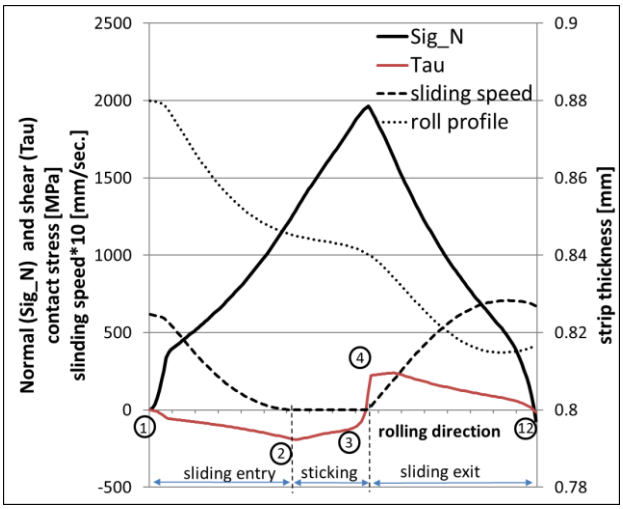

Figure 17. roll bite description: the different zones (sliding entry, sticking central and sliding exit

zones), roll profile and contact stresses. Simulation conditions: trial #5 (strip elongation = 7.8%).

The model considers that the ploughing of the strip roughness by the roll is created by the roll-strip sliding at the exit of the roll bite only. This is because in this exit zone, the roll-strip contact pressure decreases progressively together with the roll-strip contact. This progressive separation of roll and strip surfaces combined with the sliding of the two surfaces creates a strong erosion of the strip peaks by the roll, as illustrated by simulation results in section 4.

The sliding zone at the entry of the roll bite is considered to have no influence on the ploughing and erosion of the strip roughness in the model because here the roll is penetrating the strip progressively (progressive indentation) while the two surfaces are getting closer to each other. So even if there is sliding between surfaces, this sliding has no influence on erosion of the strip surface. Moreover, figure 18 shows that the sliding length at entry (distance 1-2) is approximately twice lower than at the exit (distance 4-5) which contributes to make entry sliding even more negligible in the ploughing mechanism.
Finally, the sticking zone in the central part of the roll bite does not have any influence on ploughing or erosion of strip surface roughness since here the interfacial sliding speed is zero so there is only indentation of roll into the strip.
To simulate the above ploughing mechanism and the associated erosion of the strip surface by the roll roughness, the strip roughness profile is indented by the roll and simultaneously shifted horizontally to reproduce the roll-strip sliding motion, considering that the contact pressure decreases at the exit of the rollgap where forward slip modifies the roughness. This ploughing mechanism is simulated with the following procedure in the model.

Procedure for ploughing computation

To illustrate the ploughing computation, the trial condition for coil #5 is considered here (fig. 18): a sliding length (strip displacement with respect to roll) is calculated along the roll bite and the corresponding contact ratio (fig.18-a).
As only exit forward slip in the roll bite contributes to the ploughing mechanism, the ploughing computation starts at the beginning of the exit sliding zone (fig. 18), at point 4 on figure 18-a. This point corresponds to the brutal drop of the contact ratio A_{net} (figure 18-b) at the beginning of the strip exit elastic zone where the strip starts to slide again with respect to the roll. From this point, 3 steps are applied to compute the ploughing mechanism.

Step 1: the total ploughing length from point 4- to roll bite exit is first determined: ploughing length = exit sliding length = length 4-12 = 57 + 63 = 120 μm for trial #5 (figure 18-a). This ploughing length is then divided in 8 segments of 15 microns each.

Step 2: the contact ratio A_{net} is then extracted from the rollgap computation of the rolling model at each of the 8 segments of step 1.
Step 3: 8 shifting steps corresponding to the 8 ploughing segments of step 1 are applied to the strip profile (horizontal displacement) to describe the progressive sliding of the strip with respect to the roll. The 8 segments are numbered from 5 to 12 on figure 18-a.
For each step, the vertical position of the strip with respect to roll is adjusted so that the contact ratio between the two surfaces is compatible with the contact ratio A_{net} from the rollgap computation of step 2.

The above 3 steps procedure made in an Excel sheet enables to simulate the sliding and progressive separation of roll from strip surface at the exit of the roll bite and its consequences on strip roughness. The next section illustrates application of this procedure on the roughness trials data.

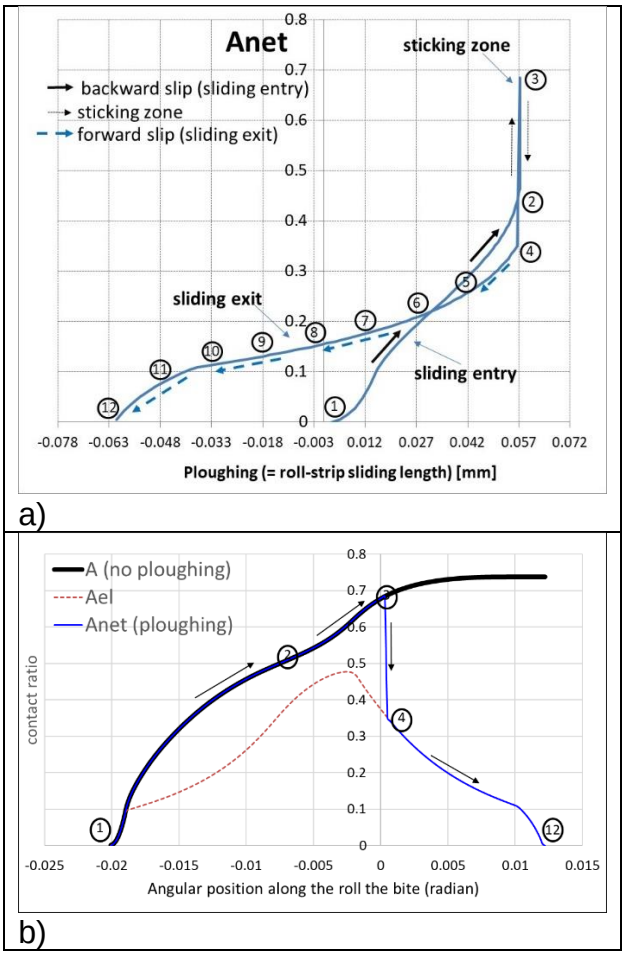

Figure 18. a) Contact ratio A_{net} versus roll-strip sliding length along the roll bite. b) evolution of the different contact ratios computed by the model along the roll bite (black arrow indicates path with ploughing). Simulation conditions: trial #5 – strip elongation=7.80%

4. MODEL APPLICATIONS

In this section, the model is applied to reproduce the roughness transfer trials conditions. Section 4.1 presents the way the model has been calibrated with trials data. Section 4.2 shows comparisons between measured and predicted roughness profiles. Section 4.3 shows application of the model to identify potential process actuators to maximize peak density on the strip after cold or temper rolling operations.

4.1 Model calibration

The rolling model for roll-gap computation has been calibrated with measured force. The strip yield stress for IF and HSLA grades has been first determined by tensile tests performed on samples taken from the coils before trials. Then the model from **[11]** has been used to determine the increase of yield stress due to the increase of strain rate coming from the rolling speed. Finally, for each rolling condition: the roll bite friction has been adjusted so that predicted and measured forces match with a difference of less than 5%.

To have a good prediction of roughness parameters measured during the trials (R_a, R_{sk}, RP_c), the asperity crushing model of Wilson **[9]** needs to be adjusted: the coefficient H (non dimensional contact pressure **[10]**) has been divided by 4 to get good results. Indeed, with the original Wilson model, the computed contact ratio A was unrealistically too high (70-100%).

4.2 Comparison model-measurements

All the trials have been simulated with the model. The trial of coil #5 is presented here: results of simulation are shown on figure 21. The progressive simulated indentation and sliding of the roll profile onto the strip surface drops dramatically the calculated strip peak density to 29, in agreement with measurements.
Figure 19 presents a zoom of figure 21: the measured and simulated strip roughness profiles are in good agreement in terms of profile characteristics: in the rolling direction (0º), the simulated profile (fig. 19-b) presents some dissymmetric peaks and valleys very similar to the measured profile (fig. 19-a). Note that the measured profile in the transverse direction (90º) does not present such dissymmetry (fig. 21 bottom).

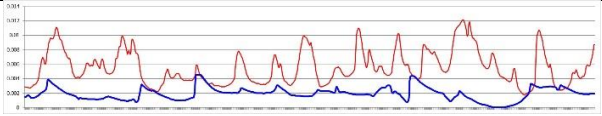

a) **Measured** profile 0º (top profile: roll, bottom profile: strip)

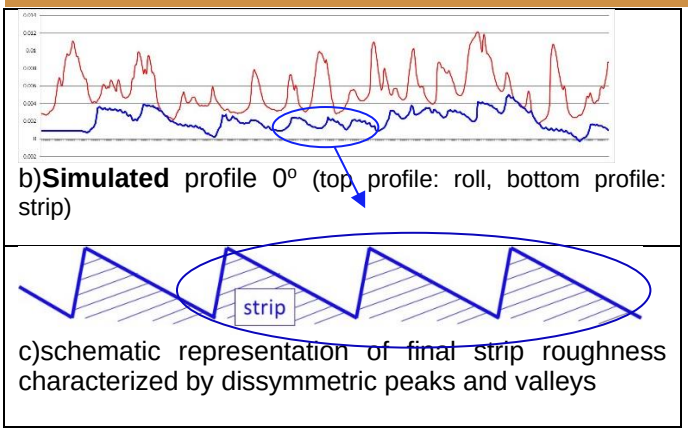

b)**Simulated** profile 0º (top profile: roll, bottom profile: strip)

c)schematic representation of final strip roughness characterized by dissymmetric peaks and valleys

Figure 19. measured and simulated final strip roughness profile characterized by dissymtric peak and valleys – rolling direction (0º) – trial #5 - 7.80%.

These differences 0º/90º are due to the ploughing mechanism as illustrated on figure 20. This mechanism is present in the rolling direction (0º) but not in the transverse direction (90º) creates dissymmetric peaks and valleys on the strip surface.

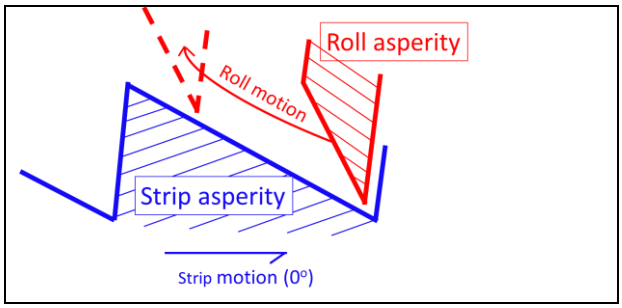

Figure 20. Illustration of progressive separation of strip from roll at the exit sliding zone producing ploughing/sliding mechanism leading to non symetric peaks/valleys on strip roughness profile.

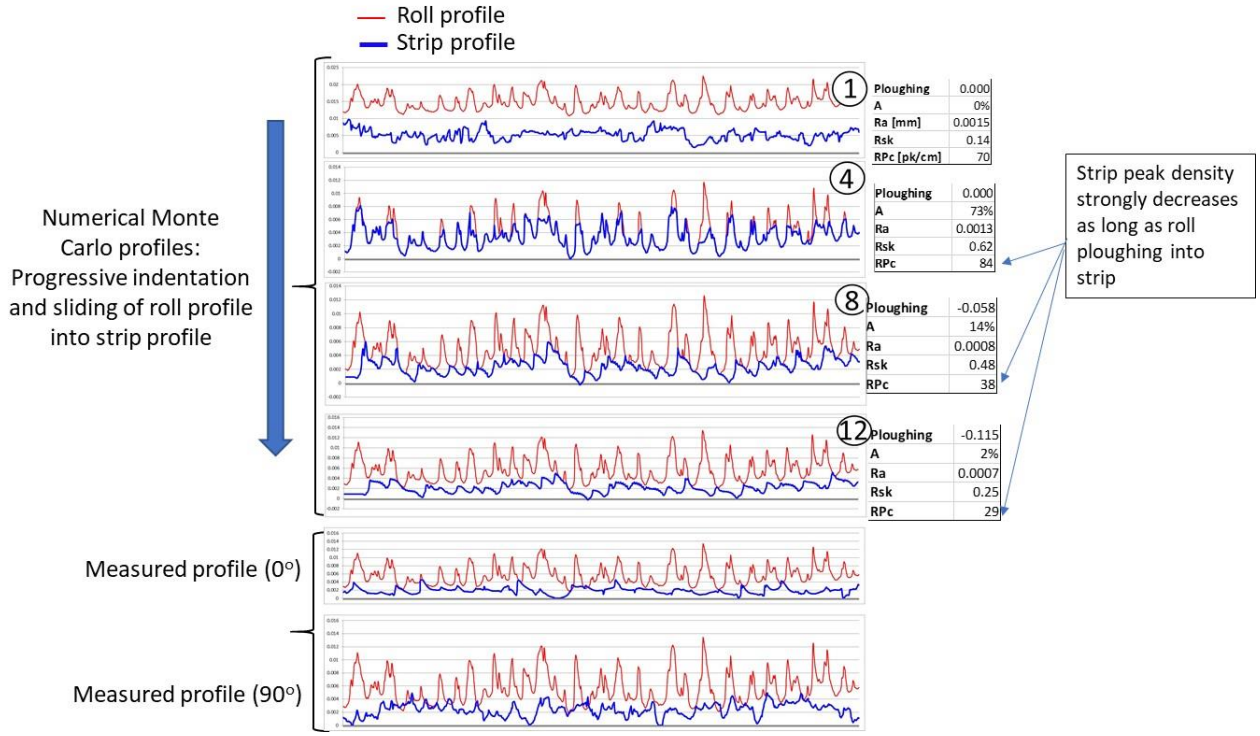

Figure 21. Trial condition #5 – Elongation=7.80%. Top: roughness transfer simulation: progressive indentation/crushing and ploughing/sliding of roll profile into strip roughness profile for the 8 shifting steps (only 3 steps are shown for better clarity). Bottom: measured roll and strip roughness profiles at 0° and 90° directions.

Figures 22, 23 and 24 presents the predicted and measured roughness parameters (R_a, R_{sk}, RP_c) for coils #3, #5, and #7 when applying the crushing and ploughing mechanisms previously exposed. The x axis is the contact ratio A varying from 0 (no contact) to 1 (complete roll-strip contact) calculated by the model, while the y axis is the measured or calculated roughness parameters (R_a, R_{sk} or RP_c). This representation presents the great interest to plot roll and strip R_a and R_{sk} at the two extremities of the horizontal axis of the graph:
-A = 0, the strip roughness is the incoming strip roughness (measured before rolling).
-A = 1 corresponds to a complete imbrication of roll into the strip so the strip has acquired the roll roughness.

Simulation results show a relatively good agreement with measured roughness for the 3 roughness parameters (R_a, R_{sk}, RP_c). However, for coil #7, the prediction of R_{sk} is not correct. This discrepancy model/measurement for the R_{sk} parameter was also observed on coils #8 and #9 (not shown here). So it seems that the R_{sk} parameter is more difficult to predict in a reliably manner than the other parameters.

These graphs show another important result about the ploughing mechanism influence:

-Figure 22: when rolls are new and strip elongation amplitude moderate, e.g. a few percents: friction in the bite is relatively high (μ=0.3) and the ploughing mechanism does not play a major roll, even for 2.91% elongation, probably because the high friction prevents from or limit the roll-strip sliding associated to the ploughing. So the roughness model with the crushing mechanism only (e.g. without the ploughing mechanism), continuous curve, describes relatively well the measured roughness, including R_{sk}.

-Figure 23: when rolls have been used for a few coils (4 coils here), roll bite friction

drops to much lower values (μ=0.15 to 0.2) which tends to activate the ploughing mechanism sooner. The ploughing seems present even at ~1% of elongation. In reality, incoming roughness between coil #3 and coil #5 is not the same since for coil #5 the strip has been previously skin passed at the inline temper mill, which is not the case for coil #3.

-Figure 24: here rolls are again new and friction is higher including for dry conditions. In that case, the ploughing mechanism seems negligible and a reasonable roughness prediction with the crushing mechanism only but (no ploughing mechanism), continuous lines, is obtained.

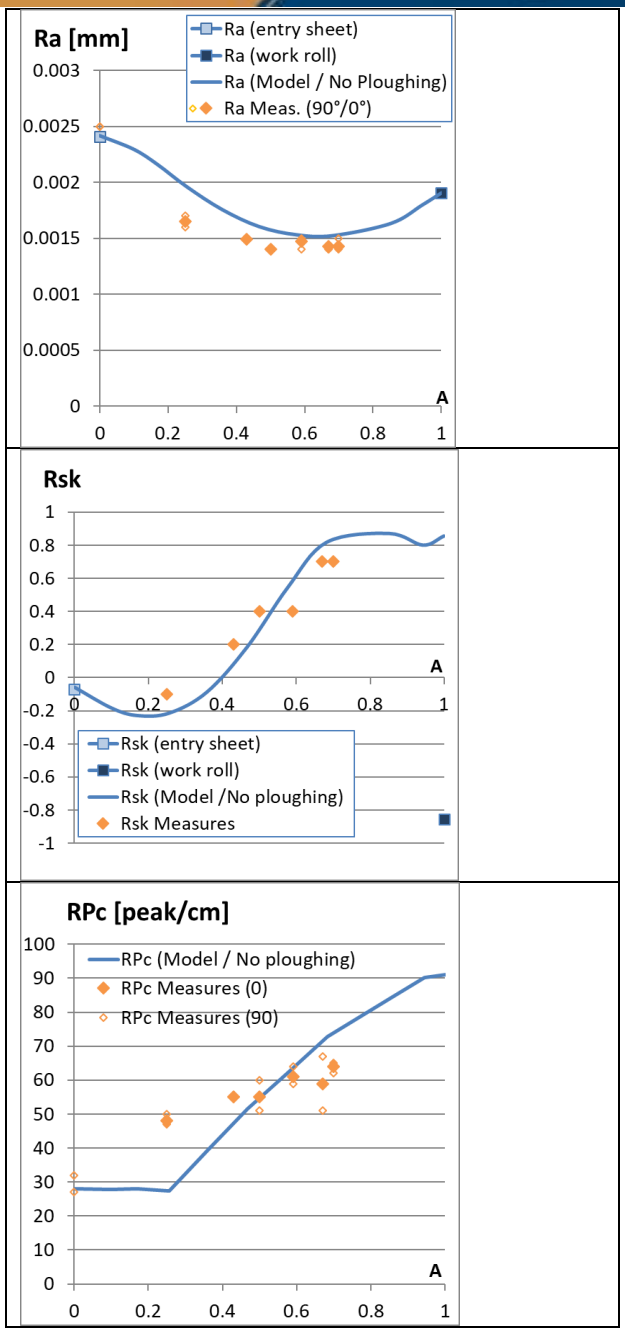

Figure 22. Trial condition coil #3 – comparison model-experiment for strip roughness Ra, Rsk, Rpc.

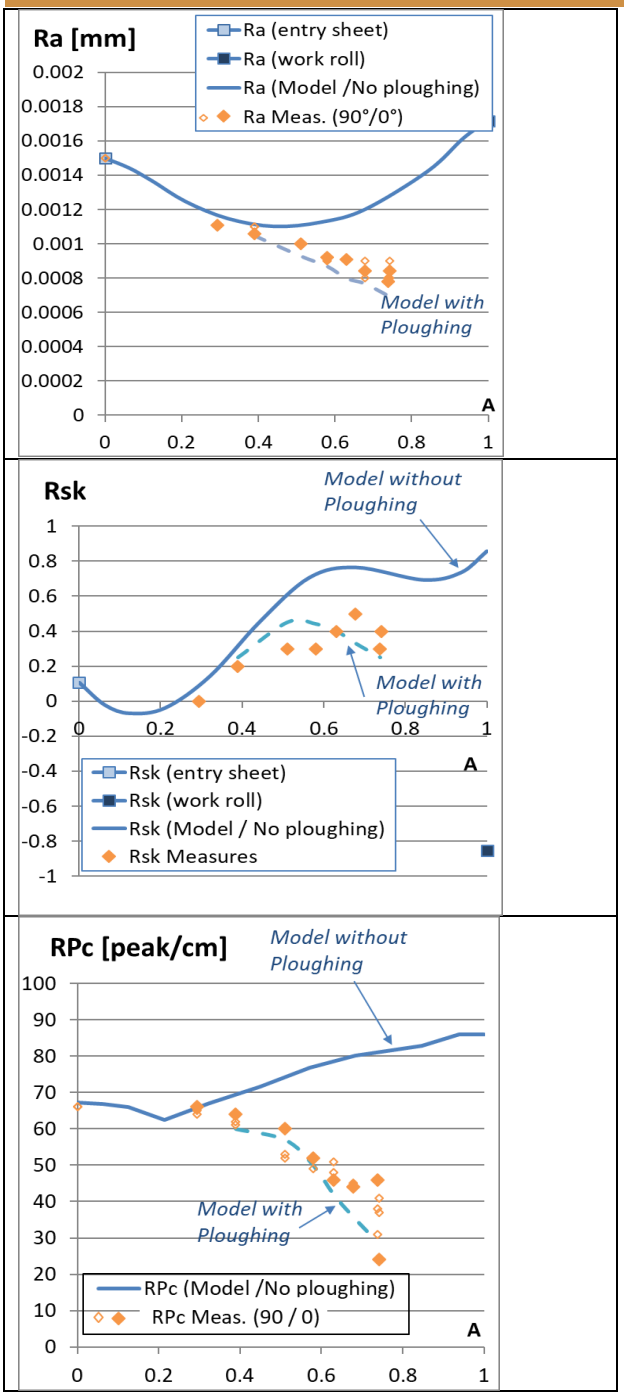

Figure 23. Trial condition coil #5 – comparison model-experiment for strip roughness Ra, Rsk, RP_c.

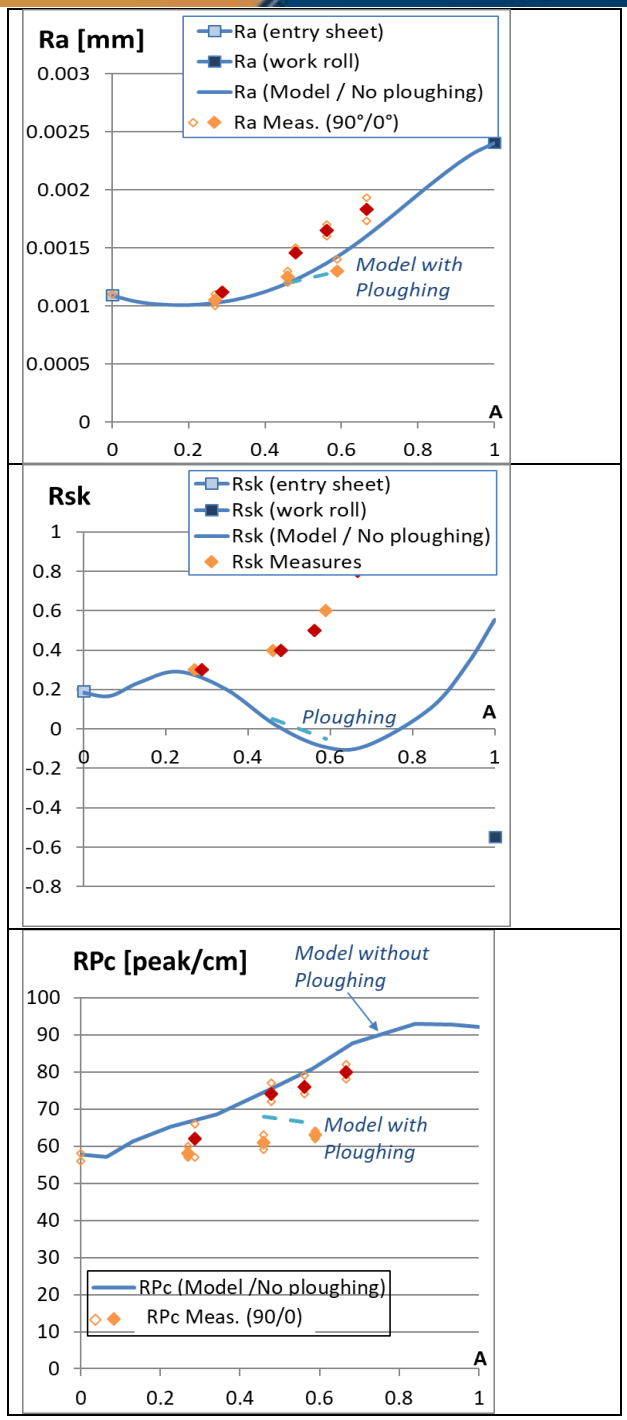

Figure 24. Trial condition coil #7 – comparison model-experiment for strip roughness Ra, Rsk, RP_c.

4.3 roughness actuators identification

Once the model has been calibrated and evaluated against experimental data, it is here used to explore possible process actuators to better control strip roughness transfer and in particular maximize the peak density on the strip after rolling. For

that purpose, three possible actuators have been explored with the model.

-increase skin pass entry peak density:

When skin pass incoming strip peak density is increased by 20 peak/cm (this can be obtained with the tandem mill last stand transfer), the model predicts that the peak density after the skin pass is increased by 10 peaks/cm for a contact ratio of 40%. 40% corresponds to a strip elongation of ~1.2% (figure 25), so there is an attenuation by a factor of 2 of the incoming strip peak density (1/2 = 10/20) (figure 25).

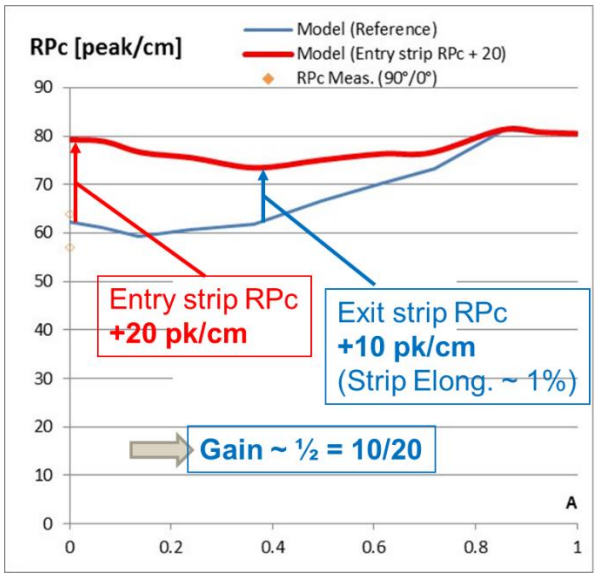

Figure 25. Influence of incoming strip peak density increase on strip roughness after skin pass (ploughing mechanism not considered to simplify). Coil #6.

-Increase skin pass roll peak density:

When the roll peak density is increased by 20 peaks/cm, the model predicts that the peak density after the skin pass is increased by 6 peaks/cm for a contact ratio of 40%. 40% corresponds to a strip elongation of ~1.2% (figure 26), so there is an attenuation by a factor of 3 (1/3 = 6/20) (figure 26).

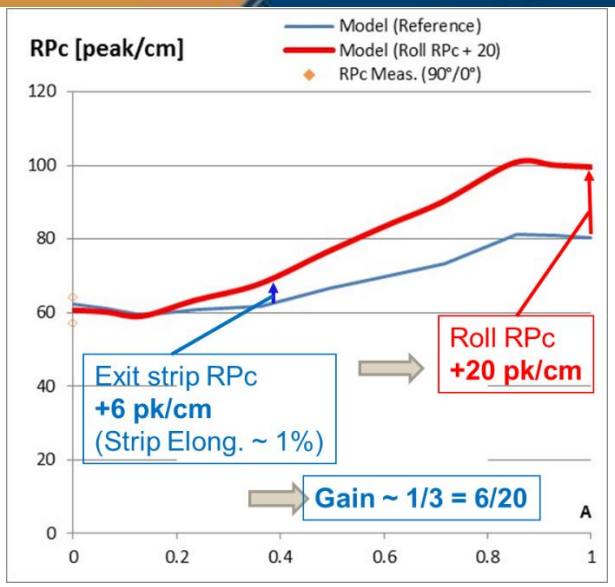

Figure 26. influence of skin pass roll peak density on strip roughness after skin pass (ploughing mechanism not considered to simplify). Coil #6.

-increase backward strip tension at skin pass and cold tandem mill:

When the entry strip tension is increased from 22 MPa to 122 MPa (so a ~5.5 factor increase), the peak density is increased from 20 to 40 peaks/cm at high elongation (7.3%) where there is ploughing. For strip elongations lower than ~3% (skin pass rolling conditions), the increase of entry strip tension seems not to play a major role in increasing peak density after skin pass (figure 27). So this actuator might not be the best one for skin pass rolling conditions.

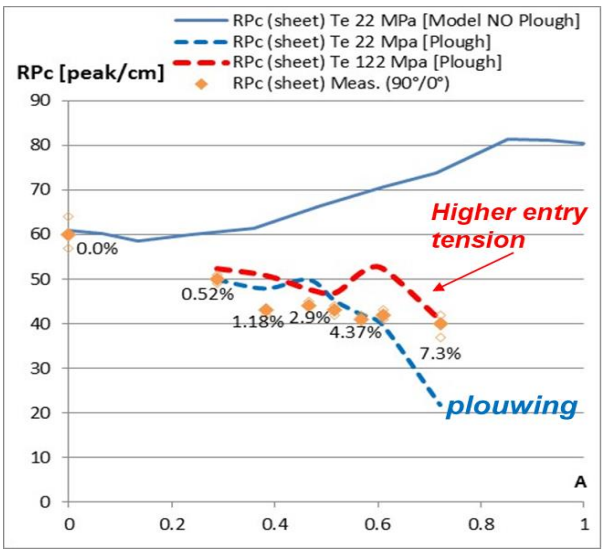

Figure 27. Influence of entry tension increase on exit strip peak density after tandem mill and skin pass (ploughing mechanism considered). Coil #5.

As a conclusion, the most efficient and most realistic actuator to maintain peak density after temper rolling as high as possible seems to be to increase peak density on the incoming strip, so increase peak density transfer at the last stand of the tandem mill.

5. CONCLUSIONS

A roughness transfer model coupled with a roll bite model has been developed to predict roughness R_a (average roughness), R_{sk} (skewness) and RP_c (peak density) after cold and temper rolling oprations. The model is based on the Monte Carlo method, the Abott curves and an auto-correlation function combined with a rolling model. Two mechanisms of roughness transfer can be considered: the crushing of asperities (strip indentation by the work roll) and the ploughing of asperities due to interfacial roll-strip sliding speed in the bite. The influence of the ploughing mechanism depends on the roll bite friction level and the strip elongation: this mechanism becomes influent at high elongation (several percents) and/or low roll bite friction. The model gives good predictions of R_a and peak density over a wide range of temper rolling conditions; the R_{sk} parameter is however for some conditions not correctly predicted. The model was also used to identify ways to improve the control of peak density after temper rolling: increase of peak density on incoming strip or work roll as well as increasing the entry strip tension are potential solutions to maintain a higher peak density on the final strip. The best and simplest solution seems to increase the incoming strip peak density at skin pass entry; this can be obtained by increasing roll peak density at the tandem mill. This model is valid only for uncoated steel sheets. To extend the model to coated steel sheets, it would be necessary to develop some roughness transfer equations for a bi-layers material composed by steel substrate and Zinc coating to be further incorporated in the roll bite model.

REFERENCES

[1] Laugier & Al. Micro-Plasto-Hydrodynamic Lubrication – a fundamental mechanism in cold rolling, Conference ICTMP, June 22-24 2014, Darmstadt, Germany.

[2] Mechanism of roughness profile transfer in skin pass rolling of thin steel strip. K. Hideo, JFE Technical Report Nº 24 (March 2019).

[3] Akashi T., Shiraishi T., Ogawa S., Matsuse Y., J. Jpn Soc. Technol. Plast., 2014 vol. 55 p.324.

[4] Akashi T., Shiraishi T., Ogawa S., Matsuse Y., Morihara, H. J., J. Jpn Soc. Technol. Plast., 2015 vol. 56 p.301.

[5] N. Legrand, C. Counhaye, D. Oliveira, Roughness Transfer Model for Cold and Temper Rolling Processes, 10th International Rolling Conference, June 06-09 2016, Graz (Austria).

[6] c. wu & Al., A new method for predicting the three-dimensional surface texture transfer in the skin pass rolling of metal strips, Wear 426-427 (2019) 1246-1264

[7]https://en.wikipedia.org/wiki/Monte_Carlo_method

[8] Patir N., Cheng H.S., J. of Lubrication Tech 100(1), 12-17 (Jan 01, 1978)

[9] W.R.D. Wilson, S. Sheu, Real Area of Contact and Boundary Friction in Metal Forming, Int. J. Mech. Sci., vol. 30 (1988) p. 475-489.

[10] Integration of roughness transfer model in a cold rolling model (in French). C. Collette, C. Counhaye, J.P. Ponthot. Published in La revue de Metallurgie-CIT, july-August 2000.

[11] Schmitz A., Herman J.C, ATB metallurgie. Modélisation et Conduite des

Procédés métallurgiques pp.37-43 (mai 1995)